PERGAMON

International Journal of Heat and Mass Transfer 42 (1999) 511–523

International Journal of HEAT and MASS TRANSFER

Optimum profiles for asymmetrical longitudinal fins in cylindrical ducts

Giampietro Fabbri*

Dipartimento di Ingegneria Energetica, Nucleare e del Controllo Ambientale, Universitá degli studi di Bologna, Italy

Received 15 January 1998; in final form 5 May 1998

Abstract

In the present work the problem of optimizing the geometry of tubes with internal asymmetrical fins in order to enhance the heat transfer under laminar flow conditions is studied. The velocity and temperature distributions on the finned tube cross-section are determined with the help of a finite element model and a global heat transfer coefficient; an equivalent Nusselt number and a compared effectiveness are calculated. Polynomial profiles are assigned to the two lateral fin surfaces and the geometry is optimized in order to make the heat transferred per unit of tube length or surface as high as possible for a given weight and for a given hydraulic resistance. The optimum asymmetrical fins, obtained by means of a genetic algorithm, are finally shown for different situations and their performances are compared with those of optimum symmetrical fins.

Nomenclature

a height of the fins [m]
c_p specific heat capacity of the coolant [J kg^{-1} K^{-1}]
E_c compared effectiveness
f_1, f_2 angular coordinate values on the fin profiles as a function of r [rad]
F_i form factors
h global heat transfer coefficient [W m^2 K^{-1}]
k_c thermal conductivity of the coolant [W m^{-1} K^{-1}]
M scale factor depending on the hydraulic resistance
n_1, n_2 fin profile polynomial orders
Nu_e equivalent Nusselt number
p generalized pressure [N m^{-2}]
q'' heat flux per unit of surface [W m^{-2}]
r radial coordinate [m]
r_i radial coordinate of the ith knot [m]
R internal radius [m]
s unfinned wall thickness [m]
t_i temperature of the ith knot [K]
T_b bulk temperature of the coolant [K]
T_c temperature of the coolant [K]
T_f temperature of the finned tube [K]
T_{max} maximum temperature on the external surface [K]
u coolant velocity [ms^{-1}]
u_i coolant velocity of the ith knot [ms^{-1}]
w_t total coolant volume flow rate [m^3 s^{-1}]
z longitudinal coordinate [m].

Greek symbols

α normalized height of the fins
β half-angle between the middle lines of two fins [rad]
γ ratio between finned tube and coolant thermal conductivity
η normalized radial coordinate
θ angular coordinate [rad]
θ_i angular coordinate of the ith knot [rad]
μ dynamic viscosity [kg m^{-1} s^{-1}]
ξ normalized area of the fin cross section
ρ coolant density [kg m^{-3}]
σ normalized unfinned wall thickness
$\bar{\sigma}$ normalized average wall thickness
ϕ_1, ϕ_2 angular coordinate on the fin profiles as a function of η [rad]
ϕ_{1i}, ϕ_{2i} fin profile describing parameters [rad]
ψ_{1i}, ψ_{2i} polynomial coefficients
ω_1, ω_2 angular coordinate values in Ω_1 and Ω_2 as a function of r [rad]
Ω_1, Ω_2 contours of the studied domain.

*Corresponding author: D.I.E.N.C.A., via Zannoni 45/2, 40134 Bologna, Italy.

0017–9310/98 $19.00
PII: S0017–9310(98)–179–3

1. Introduction

Finned surfaces are commonly used in many engineering sectors to enhance heat transfer. Many researchers have studied the problem of optimizing the shape of the finned surfaces in order to increase heat transfer effectiveness and reduce the dimensions and the weight of thermal dissipator systems. The need to reduce the volume and the weight of heat dissipators, in fact, has become even more important in many engineering fields. In the electronic industry [1–2] or in the compact heat exchanger sector [3] for example, even higher heat fluxes have to be removed from miniaturized components through very small heat transfer surfaces.

Since 1920 a variety of fin profiles have been studied in order to maximise the heat flux removed through finned surfaces [4–9]. Parabolic, triangular, undulate profiles have been proposed for longitudinal fins. Some of them have been demonstrated as having a noticeably improved effectiveness under particular conditions [10–13], but for many situations a definitive solution to the problem of optimizing the profile of the fin has not yet been found.

The heat transfer effectiveness of finned surfaces depends on different factors concerning fin conductance, the extension of the heat transfer surface between the solid and the fluid, and the local heat transfer coefficient. Each of these factors often depends on the others. For a given value of the thermal conductivity of the fin material, in order to enhance the conductance of the fins, it is necessary to increase the thickness and reduce the height. To increase the heat transfer surface, the extension of the fin must be augmented and, if the material or weight which is available for the fin is constrained, the fin thickness must be reduced. Moreover, the local heat transfer coefficient depends on the shape and the spacing of the fins in different ways.

In a previous work [14] we studied the problem of optimizing the lateral profile of longitudinal symmetrical fins located in cylindrical tubes and cooled by a fluid in laminar flow. We demonstrated that, under such conditions, the local heat transfer coefficient on the surface of the fin and of the tube wall is very sensitive to the fluidodynamic conditions determined by the fin profile. As a consequence, the improvements in the internally finned tube heat transfer effectiveness, which can be obtained by optimizing the fin profile, depend much more on the increase of the local heat transfer coefficient than on the fin surface extension or conductance enhancement.

Most of the studies performed on the optimization of the fin shape consider longitudinal fins which have symmetrical lateral profiles. This assumption simplifies the treatment of the problem with regard to the boundary conditions assignment and, if the solution is obtained in a numerical way, to the extension of the studied domain. Nevertheless, the adoption of symmetrical fins does not represent the best solution in terms of heat transfer effectiveness, mainly when the fin volume is constrained and the local heat transfer coefficient is very sensitive to the profiles of the fins. Asymmetrical fins, in fact, provide a more extended heat transfer surface for a given volume and allow more appropriate shapes of the channels between the fins to be obtained. In the present work, we then study the problem of optimizing the lateral profiles of asymmetrical fins located in cylindrical tubes and cooled by a fluid in laminar flow, in order to maximize the heat dissipated per unit of tube length or surface. As observed in the previous work [14], the case of laminar flow is interesting when the coolant velocity must be reduced, for example, in order to lower the noisiness of the devices, to avoid excessive power dissipations or to prevent miniaturized structures from large pressure gradients.

2. The mathematical model

In a cylindrical coordinate system let us consider an internally finned tube, whose axis is coincident with the z axis. All fins are asymmetrical and identical (Fig. 1a). A heat flux q'' is uniformly imposed on the external surface. Moreover, a coolant passes through the tube in laminar flow.

Since all the fins are identical, the heat transfer performances of the system can be determined by studying a portion of it delimited by the lines Ω_1 and Ω_2 which pass through the middle points of two adjacent fins as shown in Fig. 1b. Let R be the internal radius of the unfinned tube wall, s the thickness, a the fin height in the radial direction and 2β the angle between Ω_1 and Ω_2. Moreover, let the angular coordinate θ be equal to $f_1(r)$ and to $2\beta - f_2(r)$ on the two lateral fin profiles, $f_1(r)$ and $f_2(r)$ being arbitrary functions of the radial coordinate r.

In steady state, if natural convection is negligible in regard to the forced one, fluid properties are uniform, viscous dissipations within the fluid are negligible and the velocity profile is completely developed, then the velocity vector u is parallel to the z axis and the coolant flow is described by the following equation:

$$\frac{1}{r}\frac{\partial}{\partial r}\left(r\frac{\partial u}{\partial r}\right)+\frac{1}{r^2}\frac{\partial^2 u}{\partial \theta^2}=\frac{1}{\mu}\frac{\mathrm{d}p}{\mathrm{d}z} \tag{1}$$

μ being the dynamic viscosity and p a generalized pressure, which includes the gravitation potential. Equation (1) must be integrated by imposing as boundary conditions that velocity is null on the contact surface between the fluid and the solid, derivative of velocity in radial direction is null in the tube center and:

$$u[r,\omega_1(r)] = u[r,\omega_2(r)] \quad \forall r \leqslant R-a \tag{2}$$

$$\left[\frac{\partial u}{\partial N}\right]_{[r,\omega_1(r)]} = \left[\frac{\partial u}{\partial N}\right]_{[r,\omega_2(r)]} \quad \forall r \leqslant R-a \tag{3}$$

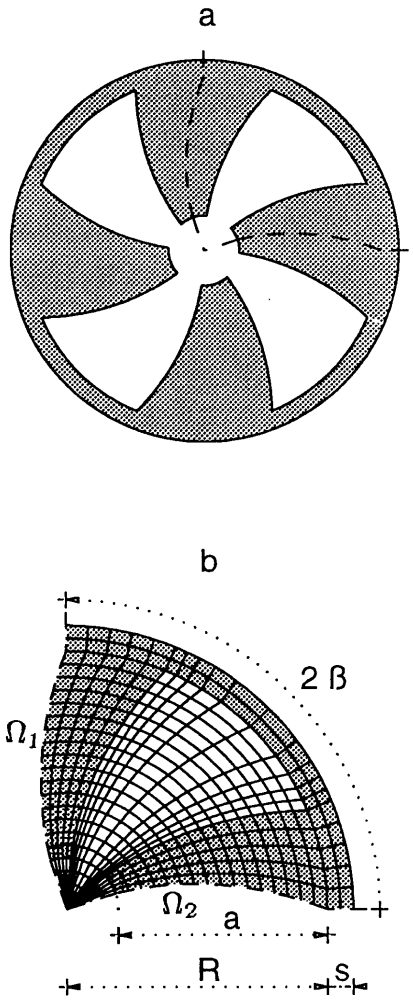

Fig. 1. Finned tube geometry: cross section (a), subdivision of a portion of the cross section in finite elements (b).

where $\omega_1(r)$ and $\omega_2(r)$ are functions which provide the value of the angular coordinate in Ω_1 and Ω_2, respectively, and N is the coordinate which is normal to the two lines.

Where the thermal profile is fully developed, the temperature distribution in the coolant is described by the following equation:

$$\frac{1}{r}\frac{\partial}{\partial r}\left(r\frac{\partial T_c}{\partial r}\right)+\frac{1}{r^2}\frac{\partial^2 T_c}{\partial \theta^2}=\frac{\rho c_p}{k_c}u\frac{\partial T_c}{\partial z} \tag{4}$$

ρ being the density, c_p the specific heat and k_c the thermal conductivity of the coolant. The temperature distribution in the finned tube is instead described by Laplace's equation:

$$\frac{1}{r}\frac{\partial}{\partial r}\left(r\frac{\partial T_f}{\partial r}\right)+\frac{1}{r^2}\frac{\partial^2 T_f}{\partial \theta^2}=0 \tag{5}$$

Equations (4) and (5) must be integrated by imposing as boundary conditions that temperature and heat flux in normal direction in fluid and solid are identical on the contact surface between fluid and solid, heat flux per unit of surface in radial direction is equal to $-q''$ on the external surface and is null in the tube center and:

$$T_c[r,\omega_1(r)] = T_c[r,\omega_2(r)] \quad \forall r \leqslant R-a \tag{6}$$

$$T_f[r,\omega_1(r)] = T_f[r,\omega_2(r)] \quad \forall R-a \leqslant r \leqslant R+s \tag{7}$$

$$\left[\frac{\partial T_c}{\partial N}\right]_{[r,\omega_1(r)]} = \left[\frac{\partial T_c}{\partial N}\right]_{[r,\omega_2(r)]} \quad \forall r \leqslant R-a \tag{8}$$

$$\left[\frac{\partial T_f}{\partial N}\right]_{[r,\omega_1(r)]} = \left[\frac{\partial T_f}{\partial N}\right]_{[r,\omega_2(r)]} \quad \forall R-a \leqslant r \leqslant R+s \tag{9}$$

Moreover, the value of the temperature in one point of the section is needed.

It is convenient to determine the velocity and temperature distributions numerically, using a finite element method [14]. The portion of the cross section of the finned tube can be subdivided in an array of elements (Fig. 1b) delimited by two concentric arches and two segments. In the center of the tube an element with the form of a circle sector can be located, supposing that in this element changes in the coolant velocity and temperature are negligible. Moreover, each element can be divided into four subelements by joining the middle points of the opposite sides.

In the first instance, let us suppose that conditions (2), (6) and (7) are not necessarily verified and momentum and heat fluxes through Ω_1 and Ω_2 are null. Moreover, let the velocity and temperature in each element be approximated by an interpolation of the values u_i and t_i, which they assume in the four knots of the element:

$$u(r,\theta)=\sum_i F_i u_i \quad T(r,\theta)=\sum_i F_i t_i \tag{10}$$

$$F_i=\frac{\ln r-\ln r_{j(i)}}{\ln r_i-\ln r_{j(i)}}\frac{\theta-\theta_{k(i)}}{\theta_i-\theta_{k(i)}} \tag{11}$$

r_i, r_j, θ_i, θ_k being knot coordinates.

From a balance between viscous and pressure forces which act on the subelements which are around each knot, the following system can then be written [14]:

$$G_M * U=\frac{1}{\mu}\frac{dp}{dz}A \tag{12}$$

where G_M is a momentum transportation matrix and U and A vectors containing the velocity of each knot and the total transversal surface of all the subelements around each knot, respectively. Moreover, from a balance between the conductive heat flux which enters the subelements around each knot and the convective heat flux in the longitudinal direction through the subelements around each knot, the following system can be written [14]:

$$G_H * T = D \tag{13}$$

$$D = \frac{q''}{k_c}\left(\frac{(R+s)2\beta}{w_t} G_A * U - L\right) \tag{14}$$

where G_H and G_A are heat transportation and surface integration matrices, respectively, L a vector containing the total perimeter crossed by q'' of the subelements around each knot, and w_t the total volume flow rate through the portion of the finned tube section. In vectors U, A, T, and L only one element has been assigned to the circular sector located at the tube center.

At this stage conditions (2) and (3) can be imposed by modifying vector U, matrix G_M and vector A in the following way:

$$\hat{U} = \begin{pmatrix} U_1 \\ U_3 \end{pmatrix} \tag{15}$$

$$\hat{G_M} = \begin{pmatrix} G_{M11} + G_{M12} + G_{M21} & G_{M13} + G_{M23} \\ G_{M31} + G_{M32} & G_{M33} \end{pmatrix} \tag{16}$$

$$\hat{A} = \begin{pmatrix} A_1 + A_2 \\ A_3 \end{pmatrix} \tag{17}$$

where index 1 and 2 refer to the knots on the lines Ω_1 and Ω_2, respectively, with the exception of that of the element at the tube center, and index 3 refers to all the other knots in fluid. By distinguishing knots on the contact surface between fluid and solid, in which velocity is known, from the others the following system is then obtained:

$$\hat{\boldsymbol{G}}_{Muu} * \hat{\boldsymbol{U}}_u = \frac{1}{\mu}\frac{dp}{dz}\hat{\boldsymbol{A}}_u \tag{18}$$

where index u refers to the knots in which the velocity is unknown. The contribution of the known velocities has been omitted since these velocities are null. By solving system (18) the velocity distribution in the portion of the conduit section is determined.

Conditions (6)–(9) can now be imposed by modifying vector T, Matrix G_H and vector D in the following way:

$$\hat{T} = \begin{pmatrix} T_1 \\ T_3 \end{pmatrix} \tag{19}$$

$$\hat{G_H} = \begin{pmatrix} G_{H11} + G_{H12} + G_{H21} & G_{H13} + G_{H23} \\ G_{H31} + G_{H32} & G_{H33} \end{pmatrix} \tag{20}$$

$$\hat{D} = \begin{pmatrix} D_1 + D_2 \\ D_3 \end{pmatrix} \tag{21}$$

where index 1, 2 and 3 refer to the same knots as in equations (14)–(16). By assigning an arbitrary temperature to a knot and distinguishing it from the others, whose temperature is unknown, the following system is then obtained:

$$\hat{\boldsymbol{G}}_{Huu} * \hat{\boldsymbol{T}}_u = \hat{\boldsymbol{D}}_u - \hat{\boldsymbol{G}}_{Hun} * \hat{\boldsymbol{T}}_n \tag{22}$$

where index n refers to the knot in which the temperature is known. By solving system (22) the temperature distribution in the portion of the cross section is determined as a function of $\hat{\boldsymbol{T}}_n$. Since the system is linear the value of this temperature does not influence the heat transfer characteristics.

Finally, the bulk temperature, the global heat transfer coefficient, the equivalent Nusselt number and the compared effectiveness can be calculated as in ref. [14]:

$$T_b = \frac{1}{w_t}\sum_i\sum_k g_{Aik} u_k t_k \tag{23}$$

$$h = \frac{q''}{T_{max} - T_b} \tag{24}$$

$$Nu_e = \frac{h2(R+s)}{k_c} \tag{25}$$

$$E_c = \frac{h2R/M}{4.364\, k_c} \tag{26}$$

where the summation index i is extended to all the knots of the coolant, g_{Aik} are the elements of matrix G_A, T_{max} is the maximum temperature, which obviously occurs on the external tube surface, and M is a scale factor which indicates how many times a finned tube with real inner radius R should be enlarged in order present the same hydraulic resistance of a flat wall tube with inner radius equal to R:

$$M = \sqrt[4]{\frac{(-dp/dz)}{\pi w_t/\beta}\Big/\frac{8\mu}{\pi R^4}} \tag{27}$$

The compared effectiveness thus results in the ratio between the heat flux dissipated by a finned tube and that removed, under the same conditions,but a flat wall tube with the same hydraulic resistance.

3. Geometry optimization

The geometry of the finned tube is described by parameters R, s, a, β and the profile functions $f_1(r)$ and $f_2(r)$. Referring s, a and the radial coordinate to the inner radius it is possible to introduce the following variable, which do not depend on the tube size:

$$\sigma = \frac{s}{R}, \quad \alpha = \frac{a}{R}, \quad \eta = \frac{r}{R}$$

$$\phi_1(\eta) = f_1(\eta R), \quad \phi_2(\eta) = f_2(\eta R) \tag{28}$$

As in ref. [14], a polynomial form can be assigned to the profile functions ϕ_1 and ϕ_2:

$$\phi_1(\eta) = \sum_{i=0}^{n_1} \psi_{1i}\eta^i \tag{29}$$

$$\phi_2(\eta) = \sum_{i=0}^{n_2} \psi_{2i}\eta^i \tag{30}$$

Such functions are univocally determined by the values which they assume in n_1+1 and n_2+1 points, which can be chosen equally spaced between the base and the tip of

the fin. Therefore, let us assume these values as fin profile describing parameters:

$$\phi_{1i} = \phi_1\left(1-\frac{i}{n_1}\alpha\right) \quad \forall i = 0, 1, \ldots, n_1 \tag{31}$$

$$\phi_{1i} = \phi_1\left(1-\frac{i}{n_2}\alpha\right) \quad \forall i = 0, 1, \ldots, n_2 \tag{32}$$

Since the behavior of the finned tube does not depend on the rotation of the coordinate system, this last can be chosen in order to let, for example, ϕ_{10} be equal to ϕ_{20}. In this way, the number of describing parameters is reduced. Moreover, two finned tubes whose cross sections are specular present the same thermal performances. To avoid redundance, the angular coordinate direction could be chosen such that, for example, the derivative of $\phi_1(\eta)$ always results positive at the beginning of the fin.

Assuming θ equal to $\phi_1(\eta)$ on a lateral fin profile and to $-\phi_2(\eta)$ on the other, the normalized area of the fin cross section ξ and the average normalized thickness of the finned tube wall $\bar{\sigma}$ are then:

$$\xi = \sum_{i=0}^{n_1} \psi_{1i}(\phi_{10},\ldots,\phi_{1n})\frac{1-(1-\alpha)^{i+2}}{i+2} + \sum_{i=0}^{n_2} \psi_{2i}(\phi_{20},\ldots,\phi_{2n})\frac{1-(1-\alpha)^{i+2}}{i+2} \tag{33}$$

$$\bar{\sigma} = \sqrt{(1+\sigma)^2+\frac{\xi}{\beta}}-1 \tag{34}$$

Parameter $\bar{\sigma}$ is representative of the solid volume of the finned tube.

The geometry optimization problem now consists in finding the combination of parameters α, β, σ, ϕ_{1i}, and ϕ_{2i} which allow the maximum Nu_e or E_c to be obtained respecting some constraining conditions. To solve such a problem a genetic algorithm [13, 15, 16] similar to that of ref. [14] can be utilized. The following variation must be introduced.

If after reproduction, the fin is too thin or too thick, parameters ϕ_{1i} or ϕ_{2i} must be resized. Let $\phi_3(\eta)$ be the sum of $\phi_1(\eta)$ and $\phi_2(\eta)$, $\phi_{3\min}$ and $\phi_{3\max}$ the minimum and the maximum values which $\phi_3(\eta)$ assumed for η between $1-\alpha$ and 1. In order to let $\phi_3(\eta)$ be no less and no greater than limit values $\theta_{\min}$ and $\theta_{\max}$, respectively, ϕ_{1i} can be changed in the following way:

$$\phi_{3i} = \begin{cases} \phi_{3\max} - \dfrac{\phi_{3\max}-\theta_{\min}}{\phi_{3\max}-\phi_{3\min}}[\phi_{3\max}-\phi_3(1-\alpha i/n_1)] \\ \quad \text{if } \phi_{3\min} < \theta_{\min} \\ \phi_{3\min} + \dfrac{\theta_{\max}-\phi_{3\min}}{\phi_{3\max}-\phi_{3\min}}[\phi_3(1-\alpha i/n_1)-\phi_{3\min}] \\ \quad \text{if } \phi_{3\max} > \theta_{\max} \end{cases} \quad \forall\ i = 0, 1, \ldots, n_1 \tag{35}$$

$$\hat{\phi}_{1i} = \phi_{1i}+\phi_{3i}-\phi_3(1-\alpha\ i/n_1) \tag{36}$$

$\hat{\phi}$ being the new parameter values.

To make the genetic algorithm faster and to avoid its stopping in correspondence with local maxima, it is expedient to maintain n_1+n_2+2 fin profile describing parameters and the redundance of specular geometries.

4. Results

Some optimizations of the finned tube geometry have been carried out in order to maximize the equivalent Nusselt number or the compared effectiveness under different conditions. In the genetic algorithm populations of 20 samples and a selection percentage equal to 20 were established and uniformly distributed between -10% and $+10\%$. Random errors were introduced during parameter reproduction. The genetic algorithm was stopped after 50 generations from the time in which an improvement was no longer observed.

Some constraints have been imposed to ensure the structural integrity of the fins and a uniform distribution of the coolant in the tube. In particular, the minimum angle between the lateral profiles of the same fin $\theta_{\min}$ has been imposed to be no less than 0.1β and the maximum $\theta_{\max}$ has been imposed to be no greater than 1.9β. Moreover, the fin height α has been constrained to an established value, which in the following optimization examples is equal to 0.8. Such a constraint has been imposed since, as observed in ref. [14], the optimization algorithm tried to extend the normalized height of the fin α as much as possible in order to create separated narrow channels. Lastly, the absolute value of the maximum difference between the values which the angular coordinate assumes on contour Ω_1 or Ω_2 has been imposed to be no greater than 2β, in order to avoid excessive rotations of the fins, which would create problems in tube production.

Finned tube geometries which maximize Nu_e are shown in Fig. 2 for n_1 equal to n_2 and ranging from 1 to 4, β equal to $\pi/4$ and γ equal to 500. A high value has been assigned to β in order to better appreciate changes in the lateral fin profiles. The value chosen for γ corresponds to the case of a finned tube made of copper and cooled by water. The characteristic parameters of the optimum geometries of Fig. 2 are reported in Table 1 together with those of the optimum geometries which will be discussed below. Geometries obtained with the genetic algorithm have been rotated in order to obtain ϕ_{10} equal to ϕ_{20}.

In the four optimum geometries, channels between the fin have comparable height, while their width increases with the polynomial order. In the first three cases the contours Ω_1 and Ω_2 present the maximum rotation which is allowed, while in the fourth case a sufficient channel width is obtained with a smaller rotation.

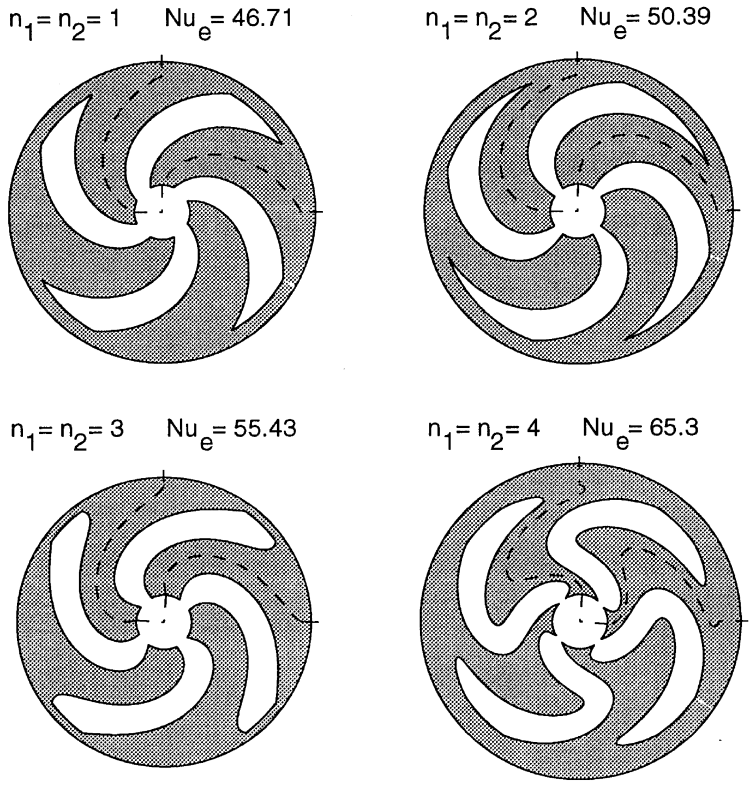

Fig. 2. Finned tube geometries which maximize Nu_e when α is equal to 0.8, β to $\pi/4$ and γ to 500.

The equivalent Nusselt numbers of the optimum geometry of Fig. 2 are considerably higher than the maximum equivalent Nusselt number which can be obtained under the same conditions with flat fins, whose lateral profile angles are constant. In particular, the equivalent Nusselt number of the tube with the optimum fourth polynomial order lateral fin profiles is more than 2.2 times that of the tube with the optimum constant profile angle, which is equal to 29.31 [14]. Moreover, the asymmetrical polynomial profile fins perform much better than the symmetrical ones of the same polynomial order. A comparison between the equivalent Nusselt number of asymmetrical and symmetrical polynomial profile fins is illustrated in Fig. 3a.

The solid volume required by the optimum geometries of Fig. 2 does not change greatly. In the first three cases, in which the channel shape is more similar, the average finned tube thickness decreases with the polynomial order.

In Fig. 4, for $\bar{\sigma}$ equal to 0.3, 0.2 and 0.1, the geometries which maximize Nu_e with asymmetrical polynomial fins of second and fourth order are compared to those with fins with zero order profiles, which are symmetrical. By constraining the average wall thickness to 0.3 and 0.2 the relative improvements of the higher order lateral fin profiles increase. Moreover, on the contrary of symmetrical fins [14], asymmetrical fins with higher order profiles still perform sensibly better than zero order profile fins even when $\bar{\sigma}$ is reduced to 0.1. A comparison between the equivalent Nusselt numbers of asymmetrical and symmetrical fin optimum geometries is illustrated in Fig. 3b for different values of the average finned tube thickness.

The equivalent Nusselt numbers of optimum geometries obtained by assigning different polynomial orders to the two lateral fin profiles are reported in Fig. 5. By varying the order of one profile the highest changes in Nu_e are observed when the order of the other profile is equal to 2.

In Figs 6 and 7 velocity and temperature distributions on the cross section of the optimized tube with asymmetrical fins are reported for polynomial order ranging from 1 to 4 and $\bar{\sigma}$ equal to 0.3. In the first case the velocity is more uniformly distributed than in the second case ($n_1 = n_2 = 2$), so that higher velocity and temperature gradients are induced between the fins, but the heat transfer surface is less extended. In the third case, velocity is less uniformly distributed between the tube center and the channels than in the second case and the heat transfer surface is less extended; but this last is better exploited

Table 1
Characteristic parameters of some optimum finned tube geometries

β	γ	n_1	n_2	$\bar{\sigma}$	σ	ϕ_{10}	ϕ_{11}	ϕ_{12}	ϕ_{13}	ϕ_{14}	ϕ_{21}	ϕ_{22}	ϕ_{23}	ϕ_{24}	Nu_e	E_c	M
$\pi/4$	500	1	1	0.346	0.103	0.5193	2.006	—	—	—	−1.133	—	—	—	46.71	3.28	2.96
$\pi/4$	500	2	2	0.344	0.114	0.3394	1.645	2.137	—	—	−0.6398	−0.9859	—	—	50.39	3.41	3.04
$\pi/4$	500	3	3	0.304	0.059	0.6297	0.9437	1.743	2.03	—	−0.083	−0.87	−0.9733	—	55.43	3.97	3.02
$\pi/4$	500	4	4	0.355	0.156	0.5945	0.8004	1.612	0.8365	0.543	−1.1071	−0.4123	−0.2487	0.7188	65.3	4.31	3
$\pi/4$	500	1	1	0.3	0.05	0.5195	1.988	—	—	—	−1.152	—	—	—	45.78	3.43	2.91
$\pi/4$	500	2	2	0.3	0.074	0.3018	1.746	2.109	—	—	−0.7785	−0.9602	—	—	48.6	3.49	2.97
$\pi/4$	500	3	3	0.3	0.053	0.5715	0.9339	1.707	2.106	—	−0.0348	−0.8418	−0.9701	—	55.25	3.96	3.04
$\pi/4$	500	4	4	0.3	0.101	0.5282	0.7871	1.589	0.7486	0.3807	−0.0859	−0.4158	−0.2141	0.7906	63.86	4.51	2.95
$\pi/4$	500	2	2	0.2	0.051	0.122	1.484	1.942	—	—	−0.8263	−1.19	—	—	33.29	3.2	2.27
$\pi/4$	500	4	4	0.2	0.05	0.3775	0.6262	1.604	0.6695	0.2007	−0.2201	−0.5201	−0.268	0.5969	47.76	4.02	2.59
$\pi/4$	500	2	2	0.1	0.053	0.0832	0.4901	1.62	—	—	−0.3183	−1.516	—	—	23.72	3.01	1.72
$\pi/4$	500	4	4	0.1	0.05	0.0894	0.3079	1.004	1.643	0.7672	−0.163	−0.7576	−1.434	−0.6825	31.19	3.53	1.93
$\pi/4$	500	2	1	0.3	0.053	0.4359	1.349	1.99	—	—	−1.15	—	—	—	46.21	3.4	2.95
$\pi/4$	500	3	1	0.3	0.073	0.2814	0.1328	−0.7862	−0.9883	—	2.128	—	—	—	52.25	3.82	2.92
$\pi/4$	500	3	2	0.3	0.087	0.5647	1.099	2.021	1.712	—	−0.7843	−0.9003	—	—	53.86	4.04	2.81
$\pi/4$	500	4	1	0.3	0.087	0.4926	0.6187	1.402	1.501	2.013	−1.083	—	—	—	54.15	4.08	2.8
$\pi/4$	500	4	2	0.3	0.077	0.6367	0.7657	1.676	1.874	2.233	−0.6492	−0.8925	—	—	60.82	4.35	2.97
$\pi/4$	500	4	3	0.3	0.083	0.6522	0.78637	1.78	1.987	2.256	−0.45	−0.9174	−0.8815	—	61.65	4.38	2.98
$\pi/4$	50	2	2	0.3	0.051	0.5241	1.332	1.949	—	—	−0.4557	−0.46154	—	—	24.39	1.88	2.83
$\pi/4$	50	4	4	0.3	0.052	0.6972	0.6334	1.189	0.5791	0.266	0.2172	0.01084	0.167	0.9659	33.62	2.41	3.04
$\pi/8$	500	2	2	0.3	0.128	0.1622	0.8015	0.9396	—	—	−0.4523	−0.5917	—	—	70.26	5.01	2.85
$\pi/8$	50	4	4	0.3	0.149	0.2409	0.3813	0.7358	0.246	0.2905	−0.0876	−0.2961	−0.1439	0.4145	87.54	6.05	2.89
$\pi/16$	500	2	2	0.3	0.211	0.0836	0.2834	0.4521	—	—	−0.2254	−0.3306	—	—	100.4	6.79	2.8
$\pi/16$	500	4	4	0.3	0.215	0.0629	0.1239	0.2516	0.0931	0.1169	−0.0245	−0.1652	−0.0733	0.2004	110.9	7.31	2.86
$\pi/4$	500	2	2	0.178	0.054	0.1117	0.9246	1.618	—	—	−0.3447	−1.522	—	—	29.13	3.16	2.
$\pi/4$	500	4	4	0.165	0.052	0.1276	0.4034	1.024	0.4099	0.4102	−0.0231	−0.3206	0.0117	−0.3046	31.18	3.25	2.09

Cases are listed in the same order they are discussed in the text.

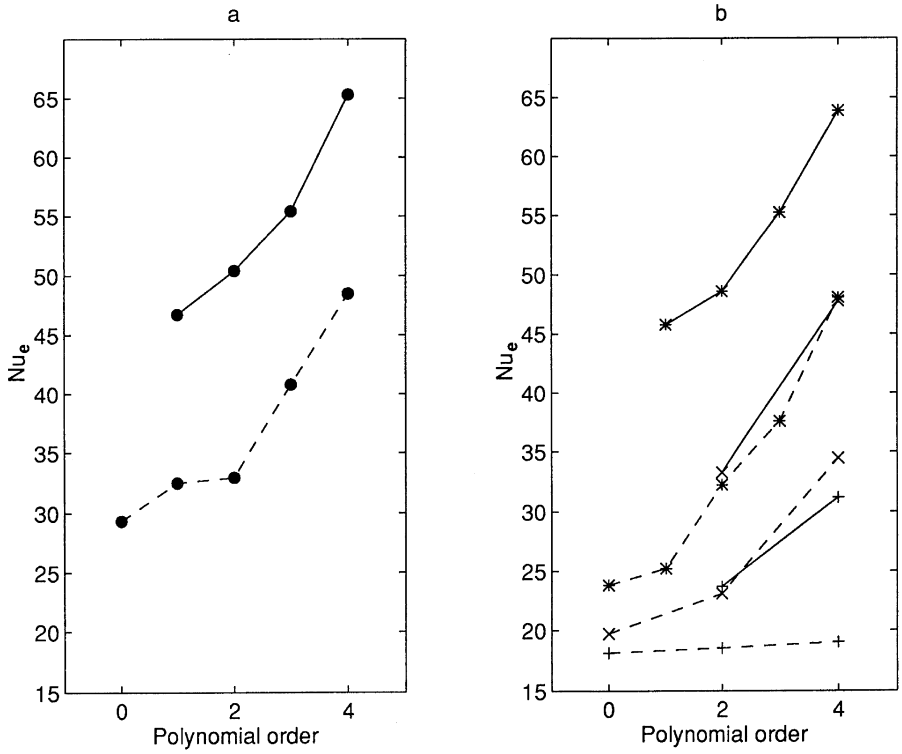

Fig. 3. Comparison between Nusselt numbers of tubes with optimum asymmetrical (continuous line) and symmetrical (dashed line) fins when $\bar{\sigma}$ is unconstrained (a) and when it is constrained (b) to 0.1 (+), 0.2 (×) and 0.3 (*).

since higher thermal gradients are induced near the tube wall and at the beginning of the fins. Lastly, in the fourth case, velocity is badly distributed compared to the previous ones and lower temperature gradients are obtained; but the wider extension of the heat transfer surface between solid and fluid provide better performances.

In Fig. 8a the equivalent Nusselt numbers of optimum geometries with asymmetrical and symmetrical fins are compared together in correspondence with two values of γ: 50 and 500. When γ is a magnitude order lower than in the previous cases the higher order profile fins still perform significantly better than the zero order ones, even if the improvements in the heat transfer are smaller. Moreover, the asymmetrical fins still present higher equivalent Nusselt numbers.

In Fig. 8b the equivalent Nusselt numbers of optimum geometries with asymmetrical and symmetrical fins are compared together in correspondence with three values of β: $\pi/4$, $\pi/8$ and $\pi/16$. It is evident that when β is equal to $\pi/8$ the fourth order asymmetrical fin still performs noticeably better than the symmetrical ones. When β is equal to $\pi/16$. since the channels between the fins become narrower, the contribution of the heat transferred through the fin tip (where velocity and temperature gradients are much higher) become more significant. As a result, the heat transfer performances of symmetrical and asymmetrical fins are less different than in previous cases. If the fin height were greater and the channel at the tube center narrower, the improvement due to the lateral fin profiles would be more noticeable.

Figure 9 shows the finned tube geometries which maximize the dissipated heat flux per unit of length with the same hydraulic resistance and solid volume of a reference unfinned tube whose wall thickness is 0.6 times its radius. The same optimum geometries also maximize the heat flux dissipated per unit of surface (i.e. $\mathbf{E}_c$) under the same conditions. Such geometries have been obtained with the genetic algorithm in the following way. Velocity distribution, hydraulic resistance and scale factor M have been determined for each describing parameter combination of the current population. The average wall thickness has then been calculated taking the solid volume of the reference tube and factor M into account. Afterward, the unfinned wall thickness has been resized in order to respect the constraint on the average tube thickness and temperature distribution has been determined. Lastly, equivalent Nusselt number or compared effectiveness have been calculated and describing parameter combinations have been selected on the basis of these parameters.

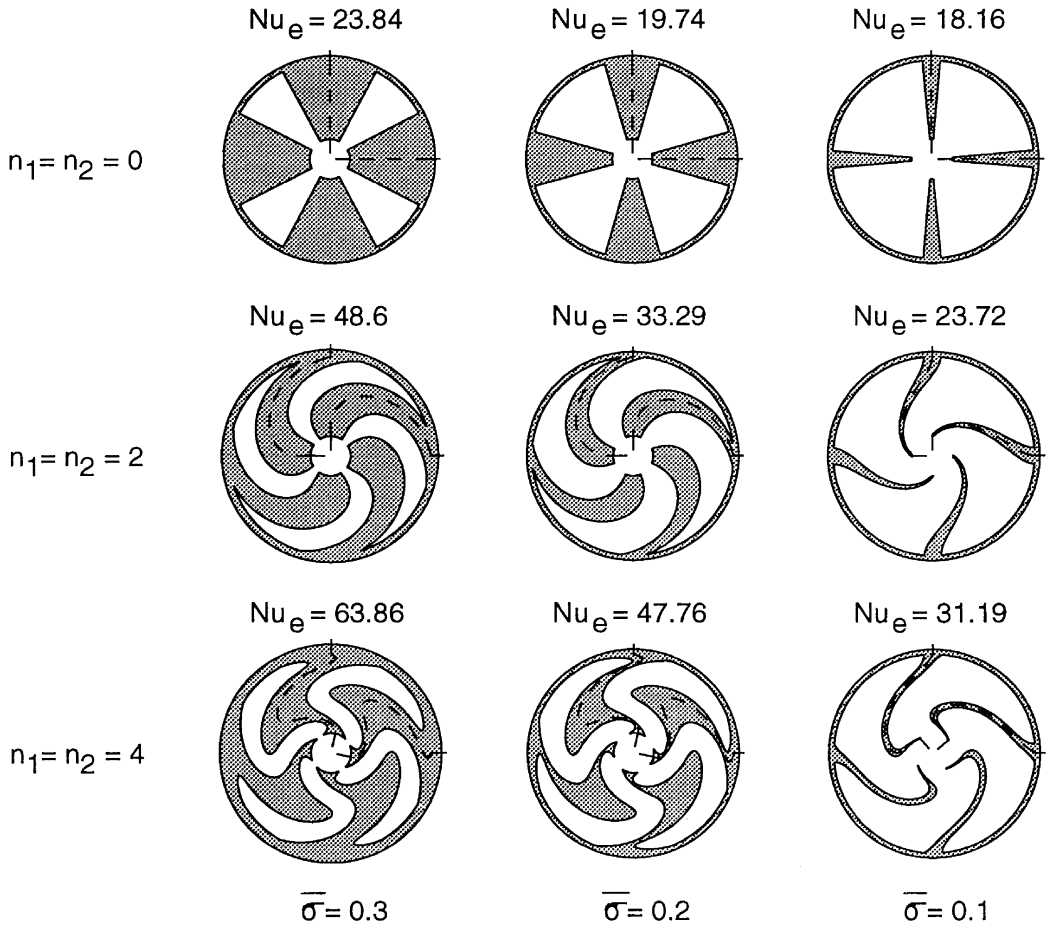

Fig. 4. Finned tube geometries which maximize Nu_e when α is equal to 0.8, β to $\pi/4$, γ to 500 and $\bar{\sigma}$ is constrained to different values.

The fourth polynomial order geometry which has been found in this way does not perform much better than the second polynomial order geometry. Anyway, it is evident that asymmetrical fins provide larger improvements in the heat transferred per unit of length or surface than symmetrical fins do [14].

5. Conclusions

The proposed mathematical model allows the heat dissipation to be studied in cylindrical tubes with internal asymmetrical fins under laminar coolant flow conditions, taking the relationship between the fin shape and the local heat transfer coefficient into account. By utilizing the model in a genetic algorithm, the geometries which maximize the heat dissipated per unit of finned tube length or surface have been found for different situations. In maximizing the dissipated heat, the consequences of constraining the solid volume or the hydraulic resistance of tubes with asymmetrical internal fins have also been investigated.

The results obtained demonstrate that, in the studied cases, asymmetrical fins perform much better than symmetrical ones, particularly with respect to fins whose lateral profile is described by a constant value of the angular coordinate. For example, in the case of a four internal fin tube made of copper and cooled by water with an average wall thickness equal to 0.3 times the internal radius, the heat flux per unit of tube length dissipated by the optimum asymmetrical fins with fourth order polynomial lateral profiles is nearly 1.33 times that removed by the optimum symmetrical fins with polynomial lateral profiles of the same order and 2.68 times that dissipated by zero polynomial order optimum fins.

Contrary to symmetrical fins, the asymmetrical ones with higher polynomial order profiles perform better than zero polynomial order fins even when the available

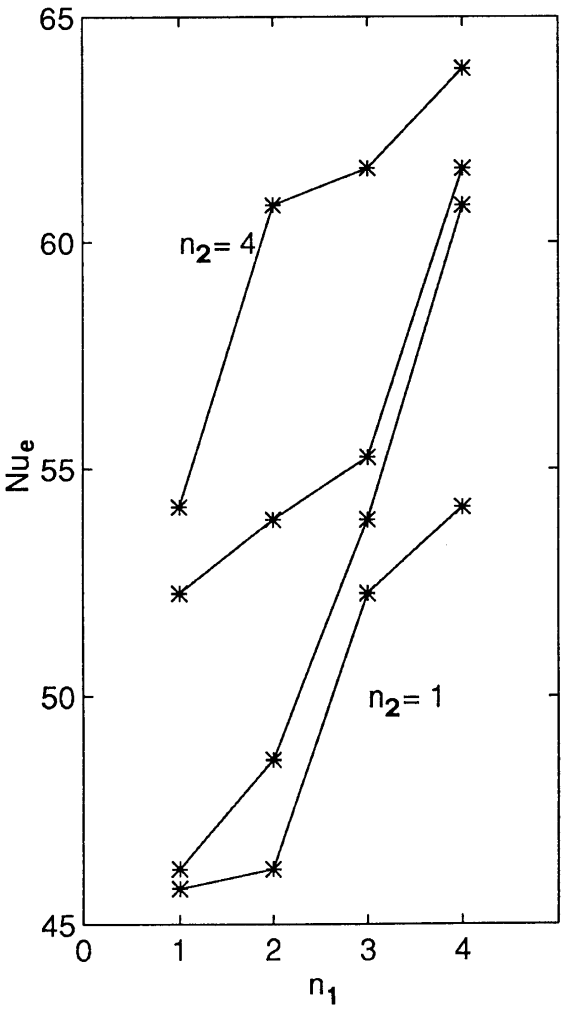

Fig. 5. Comparison between Nusselt numbers of tubes with optimum fins whose polynomial profiles have different order.

material is very scarce. The improvements in the heat transfer effectiveness of higher order asymmetrical fins decrease when the ratio between thermal conductivity of the solid and of the fluid is reduced and when the number of fins increases, in the same manner as for symmetrical fins [14].

In terms of heat flux dissipated per unit of tube length or surface for given available material and hydraulic resistance, the performances of second and fourth order fins are not very different. Second order asymmetrical fins dissipate heat fluxes which already are nearly 1.5 times those removed by zero order fins under the same conditions.

While the improvements in the heat transfer effectiveness of higher order symmetrical fins depend mainly on the increase of the local heat transfer coefficient induced by the more articulated fin shape, the improvements of higher order asymmetrical fins are a consequence of the extension of the heat transfer surface and of its better exploitation.

Tubes with asymmetrical fins, as well as with symmetrical fins, can be produced by extrusion of melted metal through an appropriate die and subsequent rectification by means of a cursor which expands the tubes and gives the final shape to the fins. In order to make the cursor motion easier, rounded corners between the fins and the tube wall are preferable. In the studied cases, fourth order polynomial profile fins, which provide the highest equivalent Nusselt numbers, also create the most rounded channels.

A more correct solution to the problem of optimizing the geometry of internally finned tube under laminar flow conditions could be obtained by taking viscous dissipations into account. For heat removal through laminar forced convection in cylindrical smooth wall ducts with uniform heat flux imposed on the external wall surface, it has been demonstrated [17, 18] that the Nusselt number calculated by considering viscous dissipations is lower than by neglecting them. In internally finned tubes, the effects of viscous dissipations are more sensible, since higher velocity gradients occur. Since the improvements in the heat transfer of symmetrical fins are related to higher velocity and temperature gradients, it is then expected that they are more affected by viscous dissipations than improvements in the heat transfer of asymmetrical fins.

It would also be interesting to study the optimization problem by considering as a boundary condition a constant temperature on the external wall surface. For laminar forced convection in internally finned tubes, analyses performed by neglecting viscous dissipation [19, 20] demonstrate that the Nusselt number is less sensitive to changes in the tube geometry when the external temperature is constant. Therefore, under such conditions, improvements in the heat transfer of polynomial fins would probably be more limited. Nevertheless, for laminar forced convection in cylindrical smooth wall ducts with constant temperature on the external wall surface, it has been demonstrated [18] that the Nusselt number calculated by considering viscous dissipations is nearly three times that obtained by neglecting them. For internally finned tubes, where higher velocity gradients occur, it is then expected that the heat transfer is strongly influenced by the alteration of viscous dissipations induced by changes in the tube geometry. Therefore,by taking viscous dissipation into account, the improvements in the heat transfer of polynomial profile fins are expected to be considerable even for the boundary condition of constant wall temperature. Moreover, optimized asymmetrical fins are expected to induce higher velocity gradients and viscous dissipations than the optimized ones found in the present analysis.

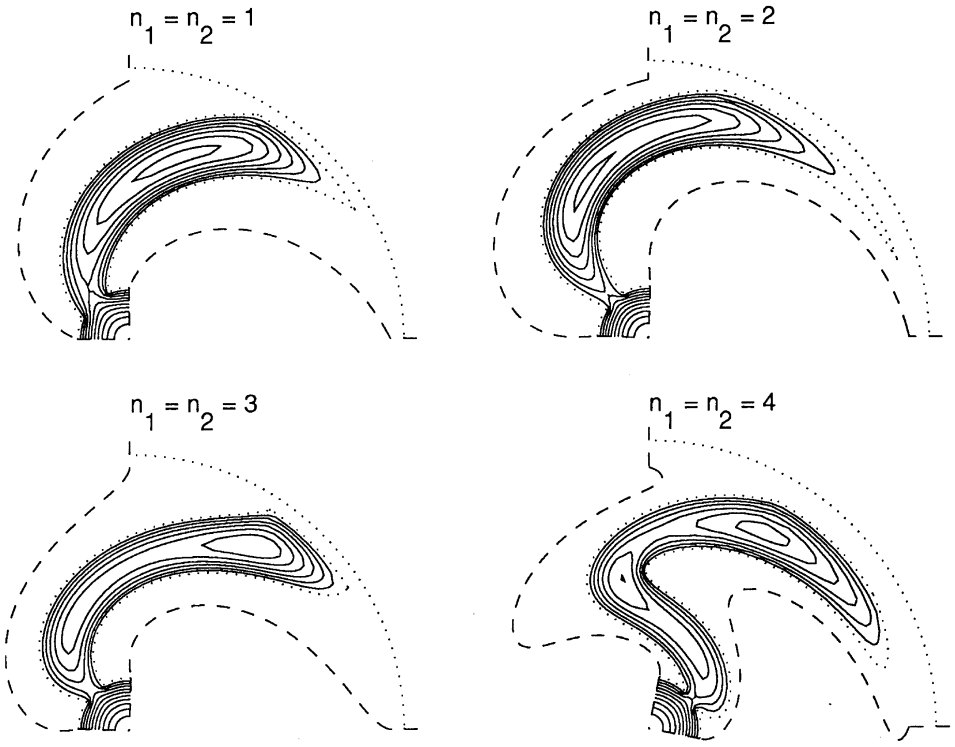

Fig. 6. Velocity distributions in the cross section of optimum tubes when α is equal to 0.8, β to $\pi/4$, γ to 500 and $\bar{\sigma}$ is constrained to 0.3. Curves are drawn every 10% of the maximum velocity.

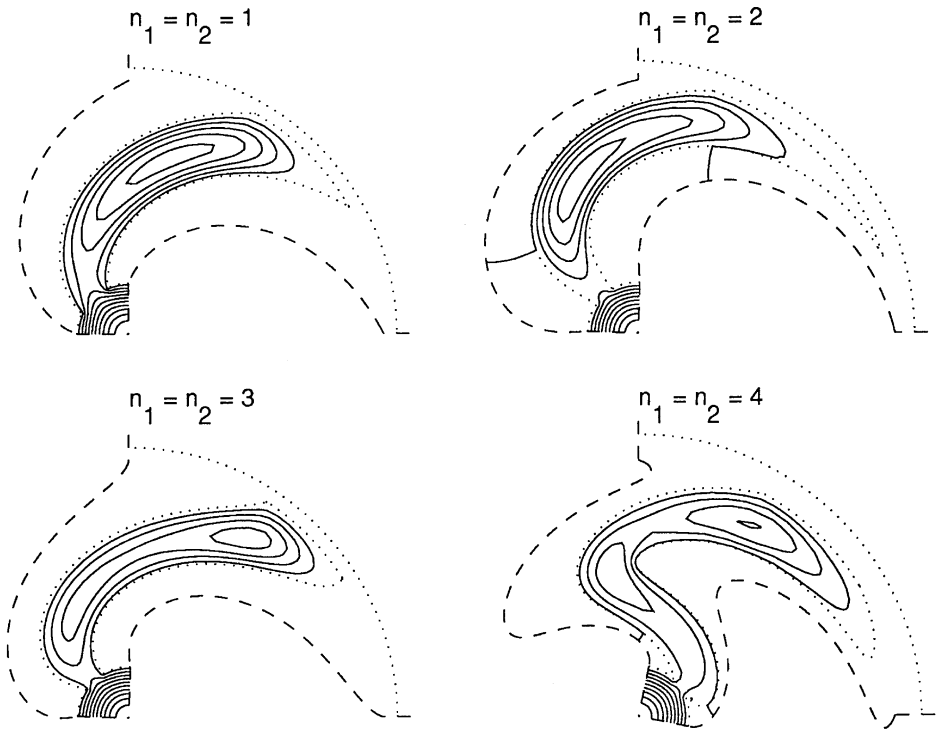

Fig. 7. Temperature distributions in the cross section of optimum tubes when α is equal to 0.8, β to $\pi/4$, γ to 500 and $\bar{\sigma}$ is constrained to 0.3. Curves are drawn every 10% of the difference between the maximum and minimum temperatures.

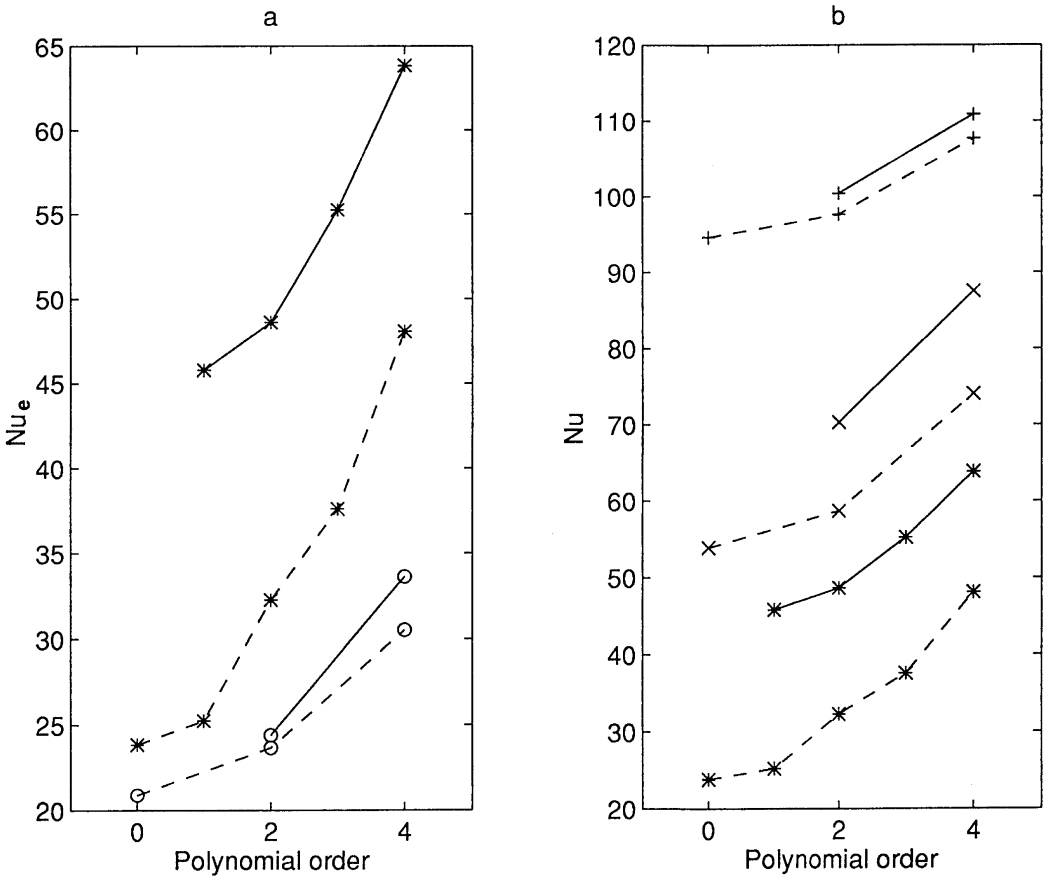

Fig. 8. Comparison between the Nusselt numbers of the tubes with optimum asymmetrical (continuous line) and symmetrical (dashed line) fins obtained by letting γ be equal to 500 (*) and 50 (0) and keeping β equal to $\pi/4$ (a) and by letting β be equal to $\pi/4$ (*), $\pi/8$ ($\times$) and $\pi/16$ (+) and keeping γ equal to 500 (b) with α equal to 0.8 and $\bar{\sigma}$ constrained to 0.3.

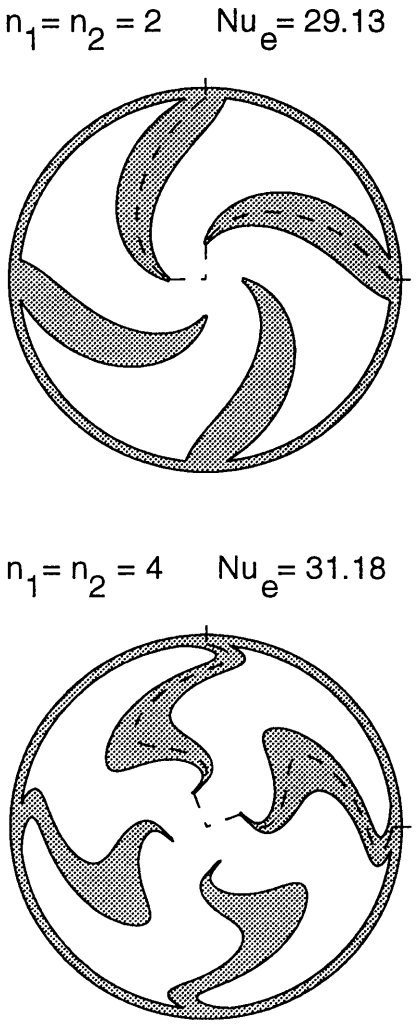

Fig. 9. Finned tube geometries which maximize the dissipated heat flux per unit of length and surface with the same hydraulic resistance and solid volume of a reference unfinned tube whose wall thickness is 0.6 times its radius.

References

[1] A. Bar-Cohen, A.D. Kraus, Advances in Thermal Modeling of Electronic Components and Systems, Vol. 2. ASME Press Series, New York, 1990, pp. 41–107.
[2] G. Cesini, R. Ricci, B. Ruggeri, Ottimizzazione di dissipatori di calore alettati per applicazioni elettroniche. Modello numerico e verifica sperimentale. Proceedings of 10th UIT National Congress, 1992, pp. 201–212.
[3] W.M. Kays, A.L. London, Compact Heat Exchangers, 3rd. ed., McGraw-Hill, New York, 1984.
[4] E. Schmidt, "Die Warmeueberragung durch Rippen", Zeitschrift des Vereines deutscher Ingenieure 70 (1926) 885–951.
[5] R.J. Duffin "A variational problem relating to cooling fins", J. Math. Mech. 8 (1959) 47–56.
[6] C.J. Maday, "The minimum weight one-dimensional straight fin", ASME J. Eng. Ind. 96 (1974) 161–165.
[7] A.D. Snider, A.D. Kraus, the quest for the optimum longitudinal fin profile, Heat Transfer Engineering 2 (1987).
[8] Y. Tsukamoto, Y. Seguchi, Shape optimization problem for minimum volume fin, Heat Transfer Japanese Research 13 (1984) 1–19.
[9] A. Aziz, A.D. Snider, Optimum design of radiating and convecting-radiating fins, Heat Transfer Engineering 17 (1996) 44–78.
[10] A.D. Snider, A.D. Kraus, S. Graff, M. Rodriguez, A.G. Kuzmierczyk, Optimal fin profiles. Classical and modern, Proceedings of 9th International Heat Transfer Conference, Vol. 4, Jerusalem, 1990, pp. 15–19.
[11] M. Spiga, G. Fabbri, Efficienza di dissipatori a profilo sinusoidale, Proceedings of 12th UIT National Congress, L'Aquila, Italy, 1994, pp. 197–204.
[12] G. Fabbri, G. Lorenzini, Analisi numerica bidimensionale di dissipatori a profile sinuspoidale, Proceedings of 13th UIT National Congress, Bologna, Italy, 1995, pp. 491–499.
[13] G. Fabbri, A genetic algorithm for fin profile optimization, Int. J. Heat and Mass Transfer 40 (9) (1997) 2165–2172.
[14] G. Fabbri, Heat transfer optimization in internally finned tubes under laminar flow conditions, Int. J. Heat and Mass Transfer 41 (10) (1998) 1243–1253.
[15] N. Queipo, R. Devarakonda, J.A.C. Humphrey, Genetic algorithms for thermosciences research: application to the optimized cooling of electronic components, Int. J. Heat and Mass Transfer 37 (6) (1994) 893–908.
[16] E. Lorenzini, M. Spiga, G. Fabbri, A polynomial fin profile optimization, Int. J. Heat and Technology 12 (1–2) (1994) 137–144.
[17] J.W. Ou, K.C. Cheng, Viscous dissipation effects on thermal entrance region heat transfer in pipes with uniform wall heat flux, Appl. Sci. Res. 28 (1973) 289–301.
[18] T. Basu, D.N. Roy, Laminar heat transfer in a tube with viscous dissipation, Int. J. Heat and Mass Transfer 28 (3) (1985) 699–701.
[19] J.H. Masliyah, K. Nandakumar, Heat transfer in internally finned tubes, ASME J. Heat Transfer 98 (1976) 257–261.
[20] H.M. Soliman, T.S. Chau, A.C. Trupp, Analysis of laminar heat transfer in internally finned tubes with uniform outside wall temperature, ASME J. Heat Transfer 102 (1980) 598–604.